Inorg. Chem. **2003**, *42*, 5900–5908

Inorganic Chemistry
Article

Oxidation Chemistry of Uranium(III) Complexes of Tpa: Synthesis and Structural Studies of Oxo, Hydroxo, and Alkoxo Complexes of Uranium(IV)

Lydia Karmazin,[†] **Marinella Mazzanti,**[*,†] **and Jacques Pécaut**[‡]

Laboratoire de Reconnaissance Ionique, Laboratoire de Coordination et Chiralité, Service de Chimie Inorganique et Biologique, FRE 2600, CEA/DSM/Département de Recherche Fondamentale sur la Matière Condensée, CEA-Grenoble, 38054 Grenoble, Cedex 09, France

Received March 19, 2003

The crystal structure of the complex $[U(tpa)_2]I_3$, **1** (tpa = tris[(2-pyridyl)methyl]amine), has been elucidated. The complex exists as only one enantiomer in the crystal leading to the chiral space group $P2_12_12_1$. The coordination geometry of the metal can be described as a distorted cube. Accidental oxidation of $[U(tpa)_2]I_3$ led to the isolation of the unusual mononuclear bishydroxo complex of uranium(IV) $[U(tpa)_2(OH)_2]I_2\cdot 3CH_3CN$, **2**, which was structurally characterized. The controlled reaction of $[U(tpa)_2]I_3$ with water resulted in the oxidation of the metal center and led to the formation of protonated tpa and of the trinuclear U(IV) oxo complex $\{[U(tpa)(\mu\text{-}O)I]_3(\mu_3\text{-}I)\}I_2$, **3**. The solid state and solution structures of this trimer are reported. The pathway suggested for the formation of this complex is the oxidation of the $[U(tpa)_2]I_3$ complex by H_2O to form a U(IV) hydroxo complex which then decomposes, eliminating mono-protonated tpa. The comparison with the reported reaction with water of cyclopentadienyl derivatives points to a higher reactivity toward water reduction of the bis(tpa) complex with respect to the cyclopentadienyl derivatives. The reaction of U(III) with methanol in the presence of the supporting ligand tpa leads to formation of alkoxo complexes similarly to what is found for amide or cyclopentadienyl derivatives. The monomethoxide complex $[U(tpa)I_3(OMe)]$, **4**, has been prepared in good yield by alcoholysis of the U(III) mono(tpa) complex. The crystal structure of this complex has been determined. The reaction of $[U(tpa)_2]I_3$ with 2 equiv of methanol in acetonitrile allows the isolation of the bismethoxo complex of U(IV) $[U(tpa)I_2(OMe)_2]$, **5**, in 35–47% yield, which has been fully characterized. To account for the oxidation of U(III) to U(IV) the suggested mechanism assumes that hydrogen is evolved in both reactions.

Introduction

Although in the past the study of the nonaqueous chemistry of uranium has mainly focused on the tetravalent oxidation state in the presence of cyclopentadienyl as the support ligand, the versatile starting material $UI_3(thf)_4$[1,2] has allowed for the preparation of an increasing number of U(III) coordination complexes with diverse ligands such as neutral N-donors,[3−7] neutral S-donors,[8] anionic N-donors,[9−14] and alkoxides.[15−17] The investigation of the electronic structure, bonding, and reactivity has been nevertheless mainly limited

---

[*] Author to whom correspondence should be addressed. E-mail: mazzanti@drfmc.ceng.cea.fr.

[†] Laboratoire de Reconnaissance Ionique.

[‡] Laboratoire de Coordination et Chiralité.

(1) Clark, D. L.; Sattelberger, A. P.; Bott, S. G.; Vrtis, R. N. *Inorg. Chem.* **1989**, *28*, 1771.
(2) Avens, L. R.; Bott, S. G.; Clark, D. L.; Sattelberger, A. P.; Watkin, J. G.; Zwick, B. D. *Inorg. Chem.* **1994**, *33*, 2248.
(3) Wietzke, R.; Mazzanti, M.; Latour, J.-M.; Pècaut, J. *J. Chem. Soc., Dalton Trans.* **1998**, 4087.
(4) Wietzke, R.; Mazzanti, M.; Latour, J.-M.; Pècaut, J. *J. Chem. Soc., Dalton Trans.* **2000**, 4167.
(5) Mazzanti, M.; Wietzke, R.; Pécaut, J.; Latour, J.-M.; Maldivi, P.; Remy, M. *Inorg. Chem.* **2002**, *2389−2399*.
(6) Berthet, J.-C.; Miquel, Y.; Iveson, P.; Nierlich, M.; Thuéry, P.; Madic, C.; Ephritikhine, M. *J. Chem. Soc., Dalton Trans.* **2002**, 3265.
(7) Rivière, C.; Berthet, J.-C.; Nierlich, M.; Ephritikhine, M.; Madic, C. *Inorg. Chem.* **2001**, *40*, 4428.
(8) Karmazin, L.; Mazzanti, M.; Pécaut, J. *Chem. Commun.* **2002**, 654.
(9) Stewart, J. L.; Andersen, R. A. *New J. Chem.* **1995**, *19*, 587.
(10) Amoroso, A. J.; Jeffery, J. C.; Jones, P. L.; McCleverty, J. C.; Rees, L.; Rheingold, A. L.; Sun, Y.; Takats, J.; Trofimenko, S.; Ward, M. D.; Yap, G. P. A. *J. Chem. Soc., Chem. Commun.* **1995**, 1881.
(11) Maria, L.; Campello, M. P.; Domingos, A.; Santos, I.; Andersen, R. *J. Chem. Soc., Dalton Trans.* **1999**, 2015.
(12) Maria, L.; Domingos, A.; Santos, I. *Inorg. Chem.* **2001**, *40*, 6863.
(13) Gambarotta, S.; Korobkov, I.; Yap, G. *Organometallics* **2001**, *20*, 2552.
(14) Roussel, P.; Scott, P. *J. Am. Chem. Soc.* **1998**, *120*, 1070.

10.1021/ic0343004 CCC: $25.00

to cyclopentadienyl derivatives,[18−30] and studies remain sparse for U(III) complexes containing different supporting ligands[13,14,16,31,32] although they are essential to gain a full understanding of the influence of the electronic and steric effects on reactivity patterns of uranium(III) complexes.

The oxidation of the metal center is a reaction well suited to study the influence of the supporting ligand on the reactivity since the high reducing power of U(III) makes uranium(III) complexes extremely reactive in oxidation reactions, and studies of the redox chemistry have been reported for different U(III) systems such as cyclopentadienyl,[22,23,26] alkoxide,[16] and triamidoamine[33] complexes. Our contribution to the study of uranium(III) chemistry has concentrated on the study of the bonding in the presence of neutral N- and S-donors.[3−5,8]

We have now begun to explore the oxidation chemistry of U(III) in the presence of the neutral tripodal N-donor tpa (tris[(2-pyridyl)methyl]amine), which provides a very different coordination environment from those cited above. We have carried out studies of the one-electron oxidation chemistry of the mono- and bis-ligand complexes $[U(tpa)I_3(MeCN)]$ and $[U(tpa)_2]I_3$[4] by water and methanol. In spite of the fact that the poor development of the coordination chemistry of uranium(III) is in part due to its exceeding sensitivity to moisture which is likely to result in the formation of hydroxide intermediates, only in very few cases has the species formed in the hydrolysis reaction been isolated and characterized. The reaction of a bis(cyclopentadienylcomplex) of U(III) with a stoichiometric amount of water leads to a U(III) complex containing bridging hydroxo groups.[29] This compound, which has been fully characterized, decomposes at high temperature to form a dimeric U(IV) oxo species. Few U(IV) metallocene hydroxides of the type Cp_3UOH have been prepared,[34] but their crystal structure has not been determined. Accidental oxidation very recently led to the structure determination of a mononuclear triamidoamine U(IV) hydroxide complex containing one terminal hydroxo group.[33]

In this paper we describe the solution and solid-state structure of the mononuclear bishydroxo U(IV) bis(tpa) complex $[U(tpa)_2(OH)_2]I_2{\cdot}3CH_3CN$ obtained by accidental hydrolysis and of the trimeric oxo U(IV) mono(tpa) complex $\{[U(tpa)(\mu\text{-}O)I]_3(\mu_3\text{-}I)\}I_2$ obtained using controlled hydrolysis conditions. We also describe the oxidation reaction of $[U(tpa)I_3(MeCN)]$ and $[U(tpa)_2]I_3$ by methanol leading to the controlled synthesis of the methoxide complexes of tpa $[U(tpa)I_3(OMe)]$ and $[U(tpa)I_2(OMe)_2]$.

Experimental Section

General Details. ^{1}H NMR spectra were recorded on Varian Mercury-400, Bruker AC-200, and Varian U-400 spectrometers using deuterated CD_3CN distilled from CaH_2 with CH_3CN as internal standard. Elemental analyses were performed under argon by Analytische Laboratorien GMBH at Lindlar, Germany.

All manipulations were carried out under an inert argon atmosphere using Schlenk techniques and a Braun glovebox equipped with a purifier unit. The water and oxygen level were always kept at less than 1 ppm. The solvents were purchased from Aldrich in their anhydrous form conditioned under argon and were vacuum distilled from K (tetrahydrofuran, isopropyl ether, hexane, methanol) or CaH_2 (acetonitrile). Depleted uranium turnings were purchased from the “Societé Industrielle du Combustible Nucleaire” of Annecy (France). Starting materials were purchased from Aldrich, and used without further purification unless otherwise stated. The ligand tris[(2-pyridyl)methyl]amine (tpa) was prepared according to the literature procedure.[35] $UI_3(thf)_4$ was prepared as described by Clark and co-workers.[2,36]

$[U(tpa)_2]I_3{\cdot}3CH_3CN$ (1). A solution of tpa (64 mg, 0.220 mmol) in CH_3CN (1.0 mL) was added to a green solution of $UI_3(thf)_4$ (100.0 mg, 0.110 mmol) in CH_3CN (1.0 mL). The resulting solution, which immediately changed color to deep purple, was left at 243 K for 1 week. A deep purple crystalline solid formed (40 mg). After filtration the mother liquor was evaporated (1.0 mL). After addition of thf (1.0 mL) and *n*-hexane a purple solid formed (45 mg) to give a total yield of 65%.

^{1}H NMR (200 MHz, CD_3CN, 298 K): δ (ppm) 0.8 (6H, s, broad, H^6), 4.3 (6H, d, H^5), 10.7 (6H, d, H^3), 12.0 (12H, s, broad, CH_2), 13.2 (6H, t, H^4).

Anal. Calcd for $[U(tpa)_2I_3]{\cdot}(CH_3CN)_3$, $UC_{42}H_{45}N_{11}I_3$: C, 38.14; H, 3.43; N, 11.65. Found: C, 37.97; H, 3.29; N, 11.76.

$[U(tpa)_2(OH)_2]I_2{\cdot}3CH_3CN$ (2). ^{1}H NMR (200 MHz, CD_3CN, 298 K): δ (ppm) -91.77 (1H, CH_2), -68.86 (1H, CH_2), -38.36 (1H, H^6), -30.29 (1H, CH_2), -20.02 (1H, H^5), -16.97 (1H, CH_2), -15.66 (1H, H^3), -11.78 (1H, H^5), -8.47 (1H, H^5), -7.94 (1H, H^4), 3.37 (1H, H^4), 12.83 (1H, H^4), 24.99 (1H, H^3), 28.08 (1H, H^3), 40.41 (1H, CH_2), 50.86 (1H, CH_2), 164.05 (1H, H^6), 169.37 (1H, H^6). Assignment of the signal was allowed by a two-dimensional $\{^1H,^1H\}$ COSY NMR correlation spectrum (relaxation delay = 0.1 s, running time of the experiment = 4 days). The experimental values of the longitudinal relaxation times of the protons in **2** are in the range 3−500 ms.

---

(15) Van Der Sluys, W. G.; Burns, C. J. *J. Am. Chem. Soc.* **1988**, *110*, 5924.

(16) Avens, L. R.; Barnhart, D. M.; Burns, C. J.; McKee, S. D.; Smith, W. H. *Inorg. Chem.* **1994**, *33*, 4245.

(17) Castro-Rodriguez, I.; Olsen, K.; Gantzel, P.; Meyer, K. *Chem. Commun.* **2002**, 2764.

(18) Brennan, J. G.; Stults, S. D.; Andersen, R. A.; Zalkin, A. *Organometallics* **1988**, *7*, 1329.

(19) Conejo, M. d. M.; Parry, J. S.; Carmona, E.; Schultz, M.; Brennan, J. G.; Beshouri, S. M.; Andersen, R. A.; Rogers, R. D.; Coles, S.; Hursthouse, M. *Eur. J. Chem.* **1999**, *5*, 3000.

(20) Burns, C. J.; Bursten, B. E. *Comments Inorg. Chem.* **1989**, *9*, 61.

(21) Pepper, M.; Bursten, B. E. *Chem. Rev.* **1991**, *91*, 719.

(22) Brennan, J. G.; Andersen, R. A. *J. Am. Chem. Soc.* **1985**, *107*, 514.

(23) Brennan, J. G.; Andersen, R. A.; Zalkin, A. *Inorg. Chem.* **1986**, *25*, 1761.

(24) Brennan, J. G.; Andersen, R. A.; Zalkin, A. *J. Am. Chem. Soc.* **1988**, *110*, 4554.

(25) Santos, I.; Pires de Matos, A.; Maddock, A. G. *Adv. Inorg. Chem.* **1989**, *34*, 65.

(26) Stults, S. D.; Andersen, R. A.; Zalkin, A. *Organometallics* **1990**, *9*, 1623.

(27) Ephritikhine, M. *New J. Chem.* **1992**, *16*, 451.

(28) Arney, D. S.; Burns, C. J. *J. Am. Chem. Soc.* **1993**, *115*, 9840.

(29) Lukens, J., Wayne W.; Beshouri, S. M.; Blosh, L. L.; Andersen, R. A. *J. Am. Chem. Soc.* **1996**, *118*, 901.

(30) Evans, W. J.; Forrestal, K. J.; Ziller, J. W. *Angew. Chem., Int. Ed. Engl.* **1997**, *36*, 774.

(31) Kaltsoyannis, N.; Scott, P. *Chem. Commun.* **1998**, 1665.

(32) Odom, A. L.; Arnold, P. L.; Cummins, C. C. *J. Am. Chem. Soc.* **1998**, *120*, 5836.

(33) Roussel, P.; Boaretto, R.; Kingsley, A. J.; Alcock, N. W.; Scott, P. *J. Chem. Soc., Dalton Trans.* **2002**, 1423.

(34) Berthet, J.-C.; Ephritikhine, M.; Lance, M.; Nierlich, M.; Vigner, J. *J. Organomet. Chem.* **1993**, *460*, 47.

(35) Anderegg, G.; Wenk, F. *Helv. Chim. Acta* **1967**, *50*, 2330.

(36) Clark, D. L.; Sattelberger, A. P.; Andersen, R. A. *Inorg. Synth.* **1997**, *31*, 307.

Table 1. Crystallographic Data for the Five Structures

	$[U(tpa)_2]I_3{\cdot}3CH_3CN$, **1**	$[U(tpa)_2(OH)_2]I_2{\cdot}3CH_3CN$, **2**	$\{[U(tpa)(\mu\text{-}O)I]_3(\mu_3\text{-}I)\}I_2{\cdot}3CH_3CN$, **3**	$[U(tpa)(OMe)I_3]$, **4**	$[U(tpa)(OMe)_2I_2]$, **5**
formula	$C_{42}H_{45}I_3N_{11}U$	$C_{42}H_{45}I_2N_{11}O_2U$	$C_{60}H_{66}I_6N_{15}O_3U_3$	$C_{19}H_{21}I_3N_4OU$	$C_{20}H_{24}I_2N_4O_2U$
fw	1322.62	1227.72	2520.77	940.13	844.26
cryst syst	orthorhombic	triclinic	monoclinic	monoclinic	monoclinic
space group	$P2(1)2(1)2(1)$	$P\bar{1}$	$P2(1)/c$	$P2(1)/n$	$P2(1)/c$
a, Å	11.9513(7)	11.4965(3)	22.1347(14)	10.4172(5)	17.6179(8)
b, Å	18.0311(11)	11.7012(3)	13.8063(9)	17.4441(8)	9.8545(4)
c, Å	22.2178(14)	17.6431(4)	25.8860(16)	12.9559(6)	15.2360(7)
α, deg	90	104.520(1)	90	90	90
β, deg	90	91.44	101.408(1)	91.002(1)	112.361(7)
γ, deg	90	91.426(1)	90	90	90
V, Å^3/Z	4787.8(5)/4	2295.67(10)/2	7754.4(9)/4	2353.97(19)/4	2446.30(19)/4
λ	0.71073	0.71073	0.71073	0.71073	0.71073
D_{calc}, g cm^{-3}	1.835	1.776	2.159	2.653	2.292
μ(Mo Kα), mm^{-1}	5.365	4.927	8.687	10.847	9.181
temp, K	193(2)	293(2)	143(2)	293(2)	193(2)
R1, wR2^a	0.0337, 0.0746	0.0269, 0.0864	0.0554, 0.1565	0.0298, 0.0660	0.0308, 0.0715

[a] Structure was refined on F_o^2 using all data: wR2 = $[\sum[w(F_o^2 - F_c^2)^2]/\sum w(F_o^2)^2]^{1/2}$, where $w^{-1} = [\sum(F_o^2) + (aP)^2 + bP]$ and $P = [\max(F_o^2, 0) + 2F_c^2]/3$.

$[U(tpa)(\mu\text{-}O)I]_3(\mu_3\text{-}I)\}I_2{\cdot}3CH_3CN$ (3). A solution of tpa (26 mg, 0.088 mmol) in CH_3CN (1.0 mL) was added to a green solution of $UI_3(thf)_4$ (40.0 mg, 0.044 mmol) in CH_3CN (1.0 mL) to obtain a deep purple solution of $[U(tpa)_2]I_3$; 1.0 mL of a 0.044 M solution of H_2O in acetonitrile (0.044 mmol) was slowly added to this solution, leading to a slow color change to yellow-brown. After 2 days the color of the solution had changed to yellow and a light brown solid had formed (20 mg, 60% yield).

IR (Nujol mull, cm^{-1}): n 1602 (s), 1308 (m), 1298 (w), 1256 (w), 1153 (m), 1087 (m), 1054 (m), 1013 (s), 964 (w), 901 (w), 755 (s, br), 721 (m), 619 (s).

^{1}H NMR (400 MHz, CD_3CN, 243 K): δ (ppm) 201.53 (1H), 127.24 (1H), 114.15 (1H), 67.02 (1H), 65.27 (1H), 58.38 (1H), 47.21 (1H), 23.95 (1H), 8.79 (1H), 6.051 (1H), −2.25 (1H), −4.41 (1H), −6.74 (1H), −10.77 (1H), −11.47 (1H), −25.97 (1H), −28.75 (1H), −86.23 (1H).

Anal. Calcd for $[U(tpa)(\mu\text{-}O)I]_3I_3{\cdot}3CH_3CN$, $U_3C_{60}H_{66}O_3N_{15}I_6$: C, 28.56; H, 2.62; N, 8.33. Found: C, 28.39; H, 2.79; N, 8.50.

Crystals suitable for X-ray diffraction were obtained in the following way.

A solution of tpa (13 mg, 0.044 mmol) in CH_3CN (0.5 mL) was added to a green solution of $UI_3(thf)_4$ (20.0 mg, 0.022 mmol) in CH_3CN (0.5 mL) to obtain a deep purple solution of $[U(tpa)_2]I_3$. The solution was transferred in an NMR tube (5 mm) equipped with a Young valve. A 1 M solution of H_2O in acetonitrile (22 μL, 0.022 mmol) was allowed to slowly diffuse into this solution from another NMR tube (5 mm) equipped with a Young valve through a sealed glass bridge connecting the two tubes. After 1 week the color of the solution changed to yellow, and brown crystals formed (11 mg, 60% yield). The proton NMR spectrum of the mother liquor shows the presence of protonated tpa.

$[U(tpa)(OMe)I_3]$ (4). A solution of tpa (16 mg, 0.055 mmol) in CH_3CN (1.5 mL) was added to a green solution of $UI_3(thf)_4$ (50.0 mg, 0.055 mmol) in CH_3CN (1.5 mL). To the resulting brown solution was added 70 mL (0.070 mmol) of a 1 M solution of MeOH in acetonitrile. The reaction mixture was left at room temperature for 2 weeks. The color of the solution changed to green, and dark emerald crystals formed (32 mg). The mother liquor was evaporated (1.0 mL), and diisopropyl ether was added (1.5 mL). After few days a green microcrystalline solid formed (5 mg, 70%). The obtained solid has a very low solubility in acetonitrile.

^{1}H NMR (200 MHz, CD_3CN, 348 K): δ (ppm) 185.30 (3H, s, $-OCH_3$), 50.24 (6H, s, broad, CH_2), 11,24 (s, broad), 9.98 (s, broad), 8.30 (s), 2.73 (s).

Anal. Calcd for $[U(tpa)(OMe)I_3]$, $UC_{19}H_{21}ON_4I_3$: C, 24.25; H, 2.23; N, 5.95. Found: C, 24.17; H, 2.33; N, 6.14.

$[U(tpa)(OMe)_2I_2]$ (5). A solution of tpa (64 mg, 0.220 mmol) in CH_3CN (1.0 mL) was added to a green solution of $UI_3(thf)_4$ (100.0 mg, 0.110 mmol) in CH_3CN (1.0 mL). To the resulting deep purple solution was added 220 μL (0.220 mmol) of a 1 M solution of MeOH in acetonitrile. The color of the solution changed to olive green. After addition of diisopropyl ether (2.0 mL) the solution was cooled at 243 K for few days to form an orange crystalline solid (30 mg, 32%). The evaporation of the mother liquor (1 mL) resulted in the formation of additional crystalline solid (35 mg) containing complex **5** as the major component, but also other U(IV) species.

^{1}H NMR (200 MHz, CD_3CN, 298 K): δ (ppm) −8.60 (3H, s, H^3), −2.50 (3H, s, H^4), 2.20 (3H, s, broad, H^6), 0.54 (3H, s, H^5), 8.67 (6H, s, broad, CH_2), 150.50 (6H, s, $-OCH_3$).

Anal. Calcd. for $[U(tpa)(OMe)_2I_2]$, $UC_{20}H_{24}O_2N_4I_2$: C, 28.45; H, 2.84; N, 6.63. Found: C, 28.60; H, 2.92; N, 6.82.

X-ray Crystallography. All diffraction data were taken using a Bruker SMART CCD area detector three-circle diffractometer (Mo Kα radiation, graphite monochromator, $\lambda = 0.71073$Å). To prevent oxidation, the crystals were coated with a light hydrocarbon oil and quickly transferred to a stream of cold nitrogen on the diffractometer.

The cell parameters were obtained with intensities detected on three batches of 15 frames with a 10 s exposure time for **1**, **2**, **3**, and **4** and 5 s for **5**. The crystal−detector distance was 5 cm. For three settings of Φ, 1273 narrow data frames, and 1041 for **4,** were collected for 0.3° increments in ω with a 10 s exposure time for **1**, **2**, **4**, and **5** and 30 s for **3**. A full hemisphere of data was collected for each complex, except for **4** which was interrupted during the data collection. At the end of data collection, the first 50 frames were re-collected to establish that crystal decay had not taken place during the collection. Unique intensities with $I > 10\sigma(I)$ detected on all frames using the Bruker SMART program[37] were used to refine the values of the cell parameters. The substantial redundancy in data allows empirical absorption corrections to be applied using multiple measurements of equivalent reflections with the SADABS Bruker program.[37] Space groups were determined from systematic absences, and they were confirmed by the successful solution of the structure (Table 1). Complete information on crystal data and data collection parameters is given in the Supporting Information.

---

(37) Bruker; Bruker, Madison, Wisconsin, USA, 1995: Madison, WI, 1995.

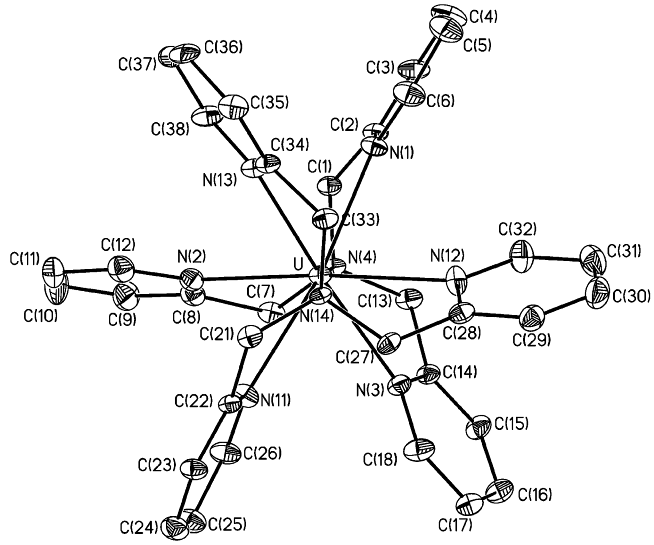

Figure 1. ORTEP diagram of the cation $[U(tpa)_2]^{3+}$, with thermal ellipsoids at 30% probability.

The structures were solved by direct methods using the SHELXTL 5.03 package.[38] For complexes **4** and **5**, all atoms, including hydrogen atoms, were found by difference Fourier syntheses. All non-hydrogen atoms were anisotropically refined on F^2, and hydrogen atoms were isotropically refined. For complexes **1**, **2**, and **3** hydrogen atoms were included in calculated positions with isotropical thermal coefficients.

Results and Discussion

As described in a previous report the reaction of $UI_3(thf)_4$ with 1 equiv of tpa leads to the mono(tpa) complex $[U(tpa)I_3X]$ (X = acetonitrile or pyridine), while the reaction of $UI_3(thf)_4$ with 2 equiv of tpa in acetonitrile leads to the formation of a bis(tpa) complex of U(III).[4] Crystals of $[U(tpa)_2]I_3$ (**1**) suitable for X-ray analysis have now been obtained by leaving standing at room temperature in a sealed vial in the drybox a $\sim 10^{-1}$ M acetonitrile (rigorously anhydrous) solution of the complex.

The ORTEP diagram of the cation $[U(tpa)_2]^{3+}$ is shown in Figure 1, and selected interatomic angles and distances are given in Table 2. The U(III) ion is eight coordinated by the nitrogens of the two tetradentate tpa ligands with the ligand arms that wrap around the metal in a pseudo-D_3 symmetric arrangement. The metal ion and the two apical tertiary amine nitrogens are aligned on the pseudo-C_3 axis (N(4)−U−N(14) = 173.0 (1)°). The two ligands show the same right-handed helical arrangement in each cation resulting in a chiral enantiomer. The complex exists as only one enantiomer in the crystal leading to the chiral space group $P2_12_12_1$. The coordination geometry of the metal can be described as a distorted cube (Figure 2) with N(11), N(2), N(3), and N(4) forming one square base (deviation from the mean plane = 0.1 Å) and N(1), N(12), N(13), and N(14) forming the opposite square plane (deviation from the mean plane = 0.1 Å) with an angle of 5.5° between the two planes. The edges of the cube are between 2.77 and 3.34 Å, and the angles within the cube described by the eight N atoms lie between 76.8° and 101.8°. Although this coordination geometry is rarely found in eight-coordinated metal complexes[39,40] for which the most commonly found geometries are square antiprismatic and dodecahedral, the same geometry has been observed for manganese(II),[41] calcium(II),[42] iron(II),[43] and mercury(II)[44] bis(tpa) complexes. The U−N distances found for the pyridyl nitrogen range from 2.595(4) to 2.621(4) Å and are only slightly longer than the ones found in the analogous U(III) complex $[U(Mentb)_2]I_3$ (Mentb = tris(*N*-methylbenzimidazol-2-ylmethyl)amine) (ranging from 2.527(6) to 2.576(6) Å).[4] Conversely the U−N distance values found for the apical tertiary amine nitrogen (2.657(4) and 2.665(4) Å) are shorter than those found in $[U[Mentb)_2]I_3$ (2.750(5) and 2.756(5) Å). The smaller difference of the values of U−N bond distances between apical nitrogen and imino nitrogen found in the bis(tpa)

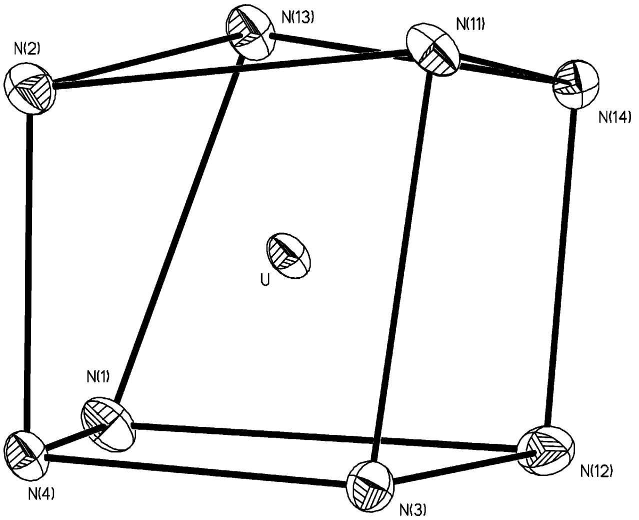

Figure 2. Coordination geometry of the cation $[U(tpa)_2]^{3+}$.

Table 2. Selected Bond Lengths (Å) and Angles (deg) for **1**

U−N(1)	2.595(4)	U−N(3)	2.608(5)
U−N(13)	2.602(5)	U−N(12)	2.621(5)
U−N(2)	2.600(5)	U−N(14)	2.657(4)
U−N(11)	2.607(5)	U−N(4)	2.665(4)

N(1)−U−N(13)	75.15(15)	N(3)−U−N(12)	72.26(16)
N(1)−U−N(2)	98.43(15)	N(1)−U−N(14)	118.27(14)
N(13)−U−N(2)	85.99(16)	N(13)−U−N(14)	63.49(14)
N(1)−U−N(11)	171.41(16)	N(2)−U−N(14)	120.68(14)
N(13)−U−N(11)	99.70(15)	N(11)−U−N(14)	63.85(14)
N(2)−U−N(11)	74.13(15)	N(3)−U−N(14)	109.73(14)
N(1)−U−N(3)	106.20(15)	N(12)−U−N(14)	63.90(15)
N(13)−U−N(3)	172.08(15)	N(1)−U−N(4)	64.07(14)
N(2)−U−N(3)	101.41(16)	N(13)−U−N(4)	123.14(14)
N(11)−U−N(3)	79.86(15)	N(2)−U−N(4)	64.09(15)
N(1)−U−N(12)	82.31(16)	N(11)−U−N(4)	114.92(14)
N(13)−U−N(12)	100.40(16)	N(3)−U−N(4)	63.49(14)
N(2)−U−N(12)	173.52(16)	N(12)−U−N(4)	110.91(15)
N(11)−U−N(12)	105.57(16)	N(14)−U−N(4)	172.99(13)

---

(38) Sheldrick, G. M. *SHELXTL 5.03*, 5th ed.; University of Göttingen: Göttingen, Germany, 1994.

(39) Kepert, D. L. *Prog. Inorg. Chem.* **1978**, *24*, 179.

(40) Lippard, S. J. *Prog. Inorg. Chem.* **1967**, *8*, 109.

(41) Gultneth, Y.; Farooq, A.; Karlin, K. D.; Liu, S.; Zubieta, J. *Inorg. Chim. Acta* **1994**, *211*, 235.

(42) Hazell, A.; McGinley, J.; Toftlund, H. *J. Chem. Soc., Dalton Trans.* **1999**, 1271.

(43) Diebold, A.; Hagen, K. S. *Inorg. Chem.* **1998**, *37*, 215.

(44) Bebout, D. C.; Ehmann, D. E.; Trinidad, J. C.; Crahan, K.; Kastner, M. E.; Parrish, D. A. *Inorg. Chem.* **1997**, *36*, 4257.

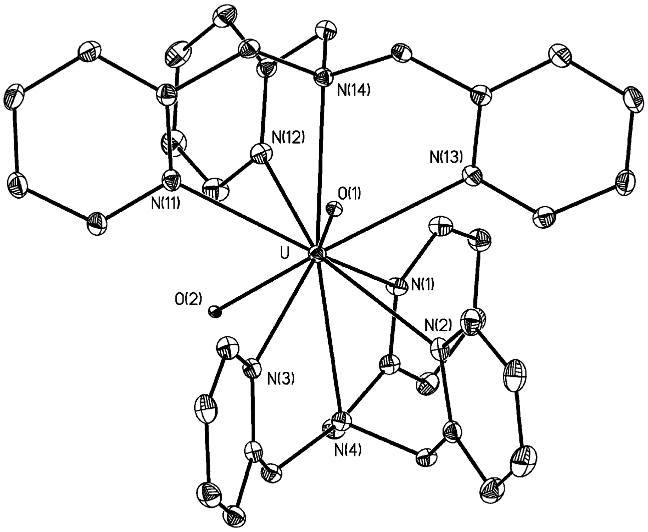

Figure 3. ORTEP diagram of the cation $[U(tpa)_2(OH)_2]^{2+}$, with thermal ellipsoids at 30% probability.

Table 3. Selected Bond Lengths (Å) and Angles (deg) for **2**

U−O(2)	2.1269(12)	U−N(13)	2.7205(18)
U−O(1)	2.1465(13)	U−N(12)	2.7336(19)
U−N(3)	2.6312(18)	U−N(4)	2.7556(19)
U−N(11)	2.633(2)	U−N(2)	2.775(2)
U−N(1)	2.719(2)	U−N(14)	2.7840(18)
O(2)−U−O(1)	134.69(5)	N(4)−U−N(14)	165.57(6)

complex with respect to the bis(Mentb) complex is also accompanied by a difference in coordination geometry (cubic for $[U(tpa)_2]^{3+}$ and bicapped trigonal antiprismatic for $[U(Mentb)_2]^{3+}$). Moreover the bis(Mentb) complex crystallizes with pairs of enantiomeric cations (same right-handed or left-handed helical arrangement of the two ligands in each cation) resulting in a racemic compound.

The complex $[U(tpa)_2]I_3$ is very reactive, and preliminary attempts to crystallize it from diluted acetonitrile solutions containing "adventitious H_2O/O_2" led repeatedly to the formation of green crystals of the U(IV) hydroxo derivative $[U(tpa)_2(OH)_2]I_2{\cdot}3CH_3CN$ (**2**). Complex **2** is the first crystallographically characterized uranium(IV) complex containing terminal hydroxides which are the only anionic ligands attached to the metal.

Structural Characterization of $[U(tpa)_2(OH)_2]I_2{\cdot}3CH_3CN$ (2). The ORTEP diagram of the cation $[U(tpa)_2(OH)_2]^{2+}$ is shown in Figure 3, and selected interatomic distances and angles are given in Table 3. The metal is 10-coordinate by two tpa ligands and two hydroxo groups, while the two iodide ions remain noncoordinating. The coordination geometry of the U(IV) is a slightly distorted bicapped square antiprism (Figure 4) with N(1), N(2), N(3), and O(2) forming one square base (deviation from the mean plane = 0.05 Å) with N(4) as the cap, and N(11), N(12), N(13), and O(1) forming the next square plane (deviation from the mean plane = 0.06 Å), N(14) being the cap. The angle between the two square planes is 5.5°. The C_3 symmetry of the tpa ligands is disrupted by the inversion of the orientation of one of the pyridine arms to fit the hydroxo groups. The two tpa ligands bend away from the hydroxo groups with an angle N(4)−U−N(14) of 165.6°. The angle between the two hydroxo oxygens is 134.7°. The value of the U−O distances (2.1269(12) and 2.1465(13) Å) similar to those found in the U(IV) triamidoamine complex $[U(NN'_3)(OH)(CH_2PMe_3)]$ ($NN'_3 = N(CH)_2CH_2NSiMe_2Bu^t)_3$) (2.145(6) Å)[33] and for terminal phenoxides in U(IV) complexes[15,45] (ranging from 2.132(8) to 2.146(4) Å) is in agreement with the assignment as U−OH and rules out the presence of oxo species (ca. 1.8 Å). This value is, as expected, shorter than those found for the bridging hydroxides in the U(III) complex $[Cp''_2U(\mu\text{-}OH)]_2$ (cp″ = $1,3\text{-}(Me_3Si)_2C_5H_3$) (2.295(3) and 2.299(3) Å).[29] The values of the distances U−N (U−N(3), 2.6312(18) Å, and U−N(11), 2.633(2) Å) for the pyridyl nitrogen which are the closest to both hydroxo groups are significantly shorter than the values found for the other pyridyl nitrogens (ranging from 2.719(2) to 2.775(2) Å) and for the apical aliphatic nitrogen (2.7556(19) and 2.7840(18) Å). The average U−N distance found for the pyridyl nitrogens (2.70(6) Å) is longer than the average $U{-}N_{py}$ distances found in the nine-coordinate complex $[U(tbpa)\ I_2]I$ (tbpa = tris[(2,2′-bipyridin-6-yl)methyl]amine) (2.63(2) Å).[3]

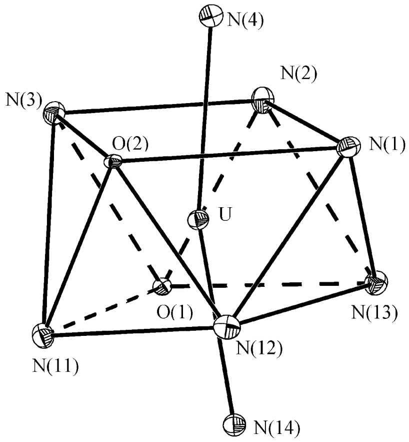

Figure 4. Coordination geometry of the cation $[U(tpa)_2(OH)_2]^{2+}$.

The proton NMR spectrum of **2** (Figure 5) in acetonitrile shows 18 signals (shifted over a very large spectral window) in agreement with the retention in solution of the C_2-symmetric axis present in the solid-state structure relating the two tpa ligands and the two hydroxo groups. A partial assignment of the NMR signals was performed by two-dimensional COSY. The signals of the hydroxo protons the closest to the metal center and the most affected by the paramagnetism of the metal ion were not found. Six signals (three sets of two connected signals) are observed for the 12 diastereotopic protons of the methylene groups, and 12 signals are found for the protons of the 6 pyridyl groups. The group of connected signals at −7.74 (H^4), −11.60 (H^5), −16.70 (H^3), and −38.00 (H^6) ppm are assigned to the pyridyl groups bent away from the hydroxo groups with long U−N distances. The other two sets of three connected signals at 28.03, 12.87, −8.28 ppm and at 24.9, 3.75, −19.7 ppm are assigned to the protons H^3, $H,^4$ H^5 of the pyridyl groups having shorter U−N bond distances. The two broad signals at 165 and 169 ppm were assigned to the protons H^6 of these

---

(45) Hitchcock, P. B.; Lappert, M. F.; Singh, A.; Taylor, R. G.; Brown, D. *J. Chem. Soc., Chem. Commun.* **1983**, 561.

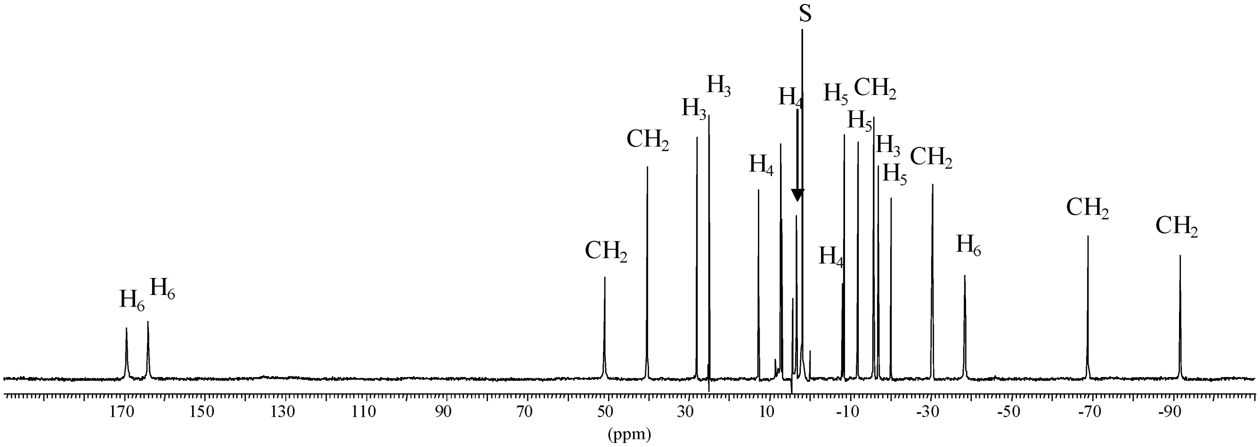

Figure 5. ^{1}H NMR spectrum in acetonitrile of the complex $[U(tpa)_2(OH)_2]I_2$.

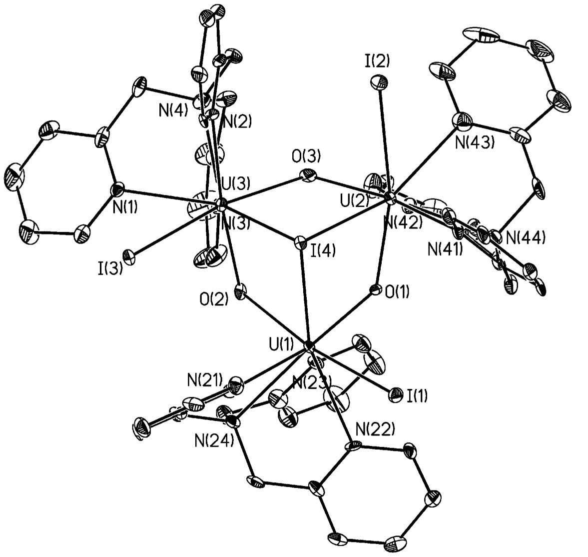

Figure 6. ORTEP diagram of the cation $\{[U(tpa)(\mu\text{-}O)I]_3(\mu_3\text{-}I)\}^{2+}$, with thermal ellipsoids at 30% probability.

Table 4. Selected Bond Lengths (Å) and Angles (deg) for **3**

U(1)−O(1)	2.069(4)	U(2)−N(44)	2.645(6)
U(1)−O(2)	2.147(4)	U(2)−N(41)	2.666(6)
U(1)−N(22)	2.625(6)	U(2)−I(2)	3.1861(6)
U(1)−N(23)	2.632(6)	U(2)−I(4	3.2840(6)
U(1)−N(24)	2.657(6)	U(2)−U(3)	3.8849(4)
U(1)−N(21)	2.659(6)	U(3)−O(2)	2.082(5)
U(1)−I(1)	3.2242(5)	U(3)−O(3)	2.146(5)
U(1)−I(4)	3.3016(6)	U(3)−N(3)	2.613(7)
U(1)−U(3)	3.8575(4)	U(3)−N(1)	2.636(6)
U(1)−U(2)	3.8938(4)	U(3)−N(2)	2.656(6)
U(2)−O(3)	2.076(5)	U(3)−N(4)	2.673(6)
U(2)−O(1)	2.166(4)	U(3)−I(3)	3.2326(6)
U(2)−N(42)	2.587(6)	U(3)−I(4)	3.2754(5)
U(2)−N(43)	2.622(7)		

O(1)−U(1)−O(2)	95.41(17)	O(1)−U(2)−U(1)	22.57(12)
O(1)−U(1)−U(3)	80.09(12)	U(3)−U(2)−U(1)	59.458(8)
O(2)−U(1)−U(3)	23.80(12)	O(2)−U(3)−O(3)	94.00(18)
O(1)−U(1)−U(2)	23.69(13)	O(2)−U(3)−U(1)	24.59(12)
U(3)−U(1)−U(2)	60.156(7)	O(2)−U(3)−U(2)	80.77(12)
O(3)−U(2)−O(1)	92.76(18)	U(1)−U(3)−U(2)	60.386(7)
O(3)−U(2)−N(41)	148.64(19)	U(1)−O(1)−U(2)	133.7(2)
O(3)−U(2)−U(3)	23.43(13)	U(3)−O(2)−U(1)	131.6(2)
O(1)−U(2)−U(3)	78.45(12)	U(2)−O(3)−U(3)	133.9(2)
O(3)−U(2)−U(1)	78.17(13)		

pyridyl groups. Their large paramagnetic shift can be explained by their close proximity to the metal ion.

Reaction of $[U(tpa)_2]I_3$ with H_2O. The NMR spectrum of solutions of $UI_3(thf)_4$ and tpa in ratio 1:2 in acetonitrile contaminated by traces of moist oxygen shows, in addition to the signals of complex **1**, a new set of signals indicating the presence of complex **2** in these partially oxidized samples.

Attempts to prepare the uranium(IV) bishydroxo complex by slow diffusion of an acetonitrile solution of 1 or 2 equiv of oxygen free H_2O into an acetonitrile solution of $[U(tpa)_2]I_3$ resulted reproductively in a slow color change to yellow accompanied by the formation of brown crystals of the trinuclear oxo complex $\{[U(tpa)(\mu\text{-}O)I]_3(\mu_3\text{-}I)\}I_2\cdot 3CH_3CN$ (**3**). The ORTEP diagram of the cation $\{[U(tpa)(\mu\text{-}O)I]_3(\mu_3\text{-}I)\}^{2+}$ is shown in Figure 6, and selected bond and interatomic distances are given in Table 4. A six-membered ring is defined by three uranium ions and three bridging oxygen atoms. The ring is capped by an iodide ion bridging across the three uranium ions. The three bridging oxo groups are located at 0.484, 0.521, and 0.534 Å below the plane of the three U(IV) ions while the bridging iodide is located at 2.41 Å above this plane. Each uranium is eight coordinate by the tpa ligand, one terminal iodide, two bridging oxides, and the bridging iodide with an irregular coordination geometry. The short U−O bond lengths ranging from 2.069(4) to 2.166(4) Å are similar to those found for $[U(C_5H_4SiMe_3)_2(\mu\text{-}O)_3]$ ranging from 2.05(1) to 2.12(1) Å and are typical for uranium alkoxide.[46] The U−O−U angles which, with a mean value of 133(1)°, are far from linear due to the trimer formation, are also similar to those found in the trinuclear cyclopentadienyl(oxo) derivative (142(2)°). The slow diffusion process takes several days, and when we started from highly concentrated solutions the coprecipitation of brown crystals of $tpaH_3I_3$ was observed. The crystal structure of this species determined by X-ray diffraction shows the presence of three protons localized on the pyridyl nitrogens as previously reported for $tpaH_3[SO_4][NO_3]$.[42]

The proton NMR spectra recorded at intermediate stages of the diffusion process did not reveal the presence of complex **2**. In addition to the signals of the starting complex **1** we observed the signals of protonated tpa showing four signals shifted downfield (doublet at 8.75 ppm (H^6), triplet

---

(46) Van Der Sluys, W. G.; Sattelberger, A. P. *Chem. Rev.* **1990**, *90*, 1027.

at 8.08 ppm (H^4), multiplet at 7.59 ppm (H^3,H^5), singlet at 4.42 ppm (CH_2)) with respect to the signals of the nonprotonated tpa (doublet at 8.49 ppm (H^6), triplet at 7.72 ppm (H^4), doublet at 7.59 ppm (H^3), triplet at 7.21 ppm (H^5), singlet at 3.84 ppm (CH_2)). The spectra also show a large number of strongly shifted NMR (−90 to 220 ppm)) signals which we were unable to assign but that suggest the presence of intermediate rigid U(IV) bis(tpa) species (by analogy with the NMR spectrum of the hydroxo complex).

Complex **3** has also been prepared in 60% yield by addition of an equivalent of H_2O to a diluted acetonitrile solution of complex **1**. The proton NMR spectrum of **3** in acetonitrile at 298 K shows only a very broad signal centered at about 0 ppm in agreement with the presence of fluxional solution species. At 243 K the proton NMR spectrum shows 18 narrow signals of equal intensity indicating the presence in solution of a rigid species in which the three pyridinyl arms of the tpa are not equivalent, as observed in the solid-state structure.

A plausible pathway for the formation of the trinuclear oxo complex is the oxidation of the $[U(tpa)_2]I_3$ complex by H_2O to form a U(IV) hydroxo complex which then decomposes, eliminating monoprotonated tpa (eq 1).

$$[U(tpa)_2]I_3 + H_2O \rightarrow [U(tpa)_2(OH)]I_3 + {}^1/_2H_2 \rightarrow {}^1/_3\{[U(tpa)(\mu\text{-}O)I]_3(\mu_3\text{-}I)\}I_2 + tpaHI \quad (1)$$

A different mechanism is also possible which involves proton transfer and metal disproportionation. However, the expected yield for this alternative pathway is lower than the observed one.

The isolation of the triply protonated $tpaH_3I_3$ can be explained by the presence of proton exchange in solution (which explains the fact that we were unable to observe an NMR signal for the rapidly exchanging H^+) and by the low solubility of this species compared to the monoprotonated species. A trinuclear structure has been observed previously for a biscyclopentadienyl(oxo) uranium(IV) complex, $[U(C_5H_4SiMe_3)_2(\mu\text{-}O)_3]$, obtained by thermal decomposition (383 K) of the corresponding triscyclopentadienyl(hydroxo) uranium(IV) species.[34] This report supports the hypothesis of a U(IV) hydroxo intermediate in the reaction of the $[U(tpa)_2]I_3$ complex with water, which appears to be more reactive than the cyclopentadienyl derivative since it decomposes at room temperature. The presence of a bis(tpa) U(IV) intermediate in this reaction is also supported by the different behavior observed in the reaction of the mono(tpa) complex with 1 equiv of water. Indeed this reaction leads to the formation of an unidentified oxidation product different from **3** without the formation of rigid asymmetric intermediate species. The reaction, reported by Andersen and co-workers, of the cyclopentadienyl derivative cp''_3U ($cp'' = 1,3\text{-}(Me_3Si)_2C_5H_3$) with water leads to a dinuclear U(III) hydroxo species which decomposes at 373 K to give the dimeric oxo species $cp''_4U_2(\mu\text{-}O)_2$. This result also points to a higher reactivity toward water reduction of the bis(tpa) complex with respect to the cyclopentadienyl derivative.[29]

Reaction of tpa Complexes of U(III) with MeOH. The addition of 1 equiv of methanol to a 10^{-2} M acetonitrile solution of the U(III) mono(tpa) complex[4] leads to a very slow color change (>3 weeks) to green and to the formation of complex $[U(tpa)I_3(OMe)]$, **4**, which can be isolated in 70% yield.

The high yield suggests that the formation of **4** proceeds according to eq 2.

$$[U(tpa)I_3] + MeOH \rightarrow [U(tpa)I_3(OMe)] + {}^1/_2H_2 \quad (2)$$

An alternative possible mechanism involving proton transfer and disproportionation would result in a much lower yield.

An analogous oxidation reaction has been observed in the alcoholysis of the U(III) species $U[N(SiMe_3)_2]_3$ with $HOSiMe_2\text{-}t\text{-}Bu$ leading to the dimeric U(IV) species $U_2(OSiMe_2\text{-}t\text{-}Bu)_8$.[47]

The addition of a small excess of methanol (0.1−0.2 equiv) accelerates the reaction without affecting the yield. However, a larger excess of methanol (1 equiv) leads to the formation of a mixture of the monomethoxo (**4**) and the bismethoxo ($[U(tpa)I_2(OMe)_2]$, **5**) U(IV) complexes and other very minor unidentified species.

For this reaction we did not observe the formation of intermediate species.

The proton NMR spectrum at 298 K of the monomethoxo complex is very broad, and only one peak at 228.5 can be clearly identified, which was assigned to the bound methoxide group, while one very broad peak is observed at 50 ppm and a group of large peaks are found between 0 and 20 ppm. At 348 K the signals become narrower although not enough to allow a complete assignment. The broad signals found for this complex indicate the presence of a slow exchange process. A large temperature dependency of the chemical shift was observed for the chemical shift of the signal assigned to the coordinated methoxide (at 185.2 at 348 K).

Emerald green crystals of complex **4** suitable for X-ray diffraction were obtained by letting stand a concentrated acetonitrile solution at room temperature.

The molecular structure of the monomethoxo complex **4** is shown in Figure 7, and selected bond distances and angles are presented in Table 5. In this complex the U(IV) ion is eight-coordinated by the tpa ligand, three iodides, and one methoxide group. The coordination polyhedron can be described as a highly distorted square antiprism. The U−N distances vary from 2.5579(19) to 2.6672(18) Å with the longest distance observed for the aliphatic nitrogen. The mean value of the U−N distances (2.61(5) Å) is similar to the one observed for the bis(tpa) complex **1** (2.62(3) Å) and only slightly shorter than the one found in the mono(tpa) complex $[U(tpa)I_3(py)]$ (2.65(2) Å). This value is significantly shorter than the average U−amine bond distances (2.79 Å) found in the only other reported U(IV) complex containing a neutral amine ligand, $[(tmed)_2U(Cl)_4]$ (tmed =

---

(47) Clark, D. L.; Sattelberger, A. P.; Van Der Sluys, W. G.; Watkin, J. G. *J. Alloys Compd.* **1992**, *180*, 303.

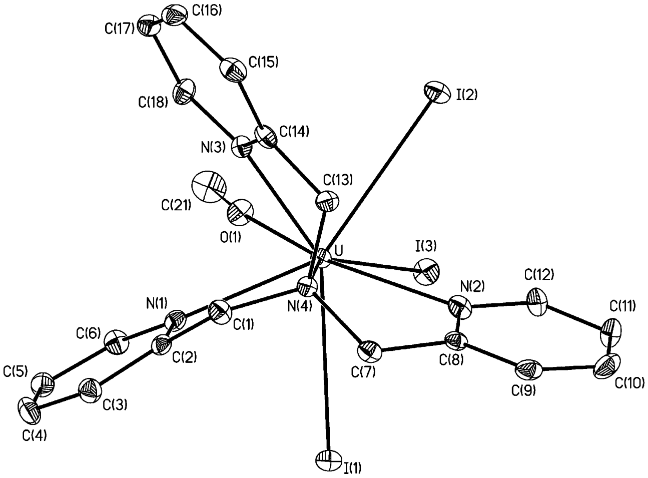

Figure 7. Top view of the molecular structure of the complex [U(tpa)(OMe)I_3], with thermal ellipsoids at 30% probability.

Table 5. Selected Bond Lengths (Å) and Angles (deg) for **4**

U−O(1)	2.0274(16)	U−N(4)	2.6672(18)
U−N(3)	2.5579(19)	U−I(3)	3.1678(2)
U−N(1)	2.5912(19)	U−I(1)	3.1776(2)
U−N(2)	2.623(2)	U−I(2)	3.1931(2)
C(21)−O(1)−U	161.28(17)		
O(1)−U−N(3)	80.64(6)	N(4)−U−I(3)	150.11(4)
O(1)−U−N(1)	77.68(6)	O(1)−U−I(1)	109.73(5)
N(3)−U−N(1)	70.95(6)	N(3)−U−I(1)	137.00(4)
O(1)−U−N(2)	162.23(7)	N(1)−U−I(1)	70.98(4)
N(3)−U−N(2)	109.99(6)	N(2)−U−I(1)	72.71(4)
N(1)−U−N(2)	118.82(6)	N(4)−U−I(1)	83.87(4)
O(1)−U−N(4)	133.98(6)	I(3)−U−I(1)	82.173(5)
N(3)−U−N(4)	62.46(6)	O(1)−U−I(2)	98.27(5)
N(1)−U−N(4)	65.36(6)	N(3)−U−I(2)	70.15(4)
N(2)−U−N(4)	63.27(6)	N(1)−U−I(2)	141.02(4)
O(1)−U−I(3)	75.80(5)	N(2)−U−I(2)	73.32(4)
N(3)−U−I(3)	139.78(4)	N(4)−U−I(2)	94.20(4)
N(1)−U−I(3)	132.70(4)	I(3)−U−I(2)	81.471(5)
N(2)−U−I(3)	87.33(4)	I(1)−U−I(2)	142.770(6)

tetramethylethylenediamine).[48] This value is also shorter than the values of the U−Nneutral (2.67(2)−2.71(0) Å) in the pentacoordinated U(IV) species [(N_3N)UX] (N_3N = N($CH_2CH_2NSiBu^tMe_2$)$_3$, X = Cl, Br, I, NEt_2)[49] containing a tripodal ligand with three anionic arms connected to a neutral amine nitrogen, but similar to the value of the U−Nneutral distance (2.624(11) Å) found for [(N_3N)UOR].[50]

The reaction of 2 × 10^{-2} M acetonitrile solutions of [U(tpa)$_2$]I_3 with 2 equiv of methanol in acetonitrile leads to an immediate color change to green and is accompanied by gas evolution (which we assume to be H_2) and formation of a precipitate which has been identified to be tpaH_3I_3 by X-ray diffraction. The proton NMR spectrum at 298 K of the reaction mixture shows at least two sets of signals, with one main species. After filtration of this mixture the slow diffusion of diisopropyl ether allows the isolation of orange crystals of the bismethoxo complex of U(IV) [U(tpa)I_2(OMe)$_2$], **5**, suitable for X-ray diffraction. The proton NMR spectrum at 298 K of the bismethoxo complex (**5**) indicates the presence of a C_{3v} symmetric solution species with one signal for the six methylene protons of the tpa ligand, four signals for the 12 pyridinyl protons, and one highly shifted (151 ppm) signal for the six protons of the two methoxide groups. The high symmetry of the solution species absent in the solid structure arises probably from the fast exchange of coordinated methoxides and iodides.

Complex **5** can be obtained pure in 35−47% yield by diffusion of diisopropyl ether into a ∼3 × 10^{-2} M solution of [U(tpa)$_2$]I_3 after the addition of 2 equiv of methanol followed by filtration of the protonated tpa. The partial evaporation of the mother liquor followed by the addition of diisopropyl ether resulted in the formation of additional crystalline solid. However, the proton NMR of this solid showed the presence of minor species, besides the bismethoxo complex **5**. One of these species, absent in the starting reaction mixture, was identified to be the monomethoxo complex [U(tpa)I_3(OMe)] (**4**), which has a lower solubility in acetonitrile than the bismethoxo complex. The crystallization of the complex **4** and other unidentified species from highly concentrated solutions arises probably from the presence under these conditions of intermolecular exchanges of iodide and methoxide ligands between species having different solubility. The intermolecular exchange of methoxide and fluoride has been described previously by Marks for the [U(OMe)$_5$F] complex.[51] This hypothesis is also supported by the presence of signals attributed to the monomethoxo complex in the proton NMR spectra of highly concentrated (>5 × 10^{-2} M) acetonitrile solutions of [U(tpa)$_2$]I_3 reacted with 2 equiv of methanol.

To account for the oxidation of U(III) to U(IV) we assume that hydrogen is evolved in the reaction

$$[\mathrm{U(tpa)_2}]\mathrm{I_3} \xrightarrow{\mathrm{MeOH}} [\mathrm{U(tpa)_2I_3(OMe)}] + {}^{1}/{}_{2}\mathrm{H_2} \xrightarrow{\mathrm{MeOH}} [\mathrm{U(tpa)I_2(OMe)_2}] + \mathrm{tpaHI} \quad (3)$$

The proton NMR spectrum of a solution of [U(tpa)$_2$]I_3 at 298 K after addition of only 1 equiv of methanol indicates the presence of unreacted [U(tpa)$_2$]I_3, of tpaHI, and of [U(tpa)I_2(OMe)$_2$]. The spectrum also shows a large number of highly shifted signals between −100 and 230 ppm in agreement with the presence of a rigid U(IV) bis(tpa) intermediate species. Attempts to isolate these species failed. The fact that these intermediate species are not observed in the reaction of the mono(tpa) complex with 1 equiv of methanol supports the mechanism given in eq 3.

The molecular structure of the bismethoxo complex (**5**) is shown in Figure 8, and selected bond distances and angles are presented in Table 6. The U(IV) ion is eight-coordinated by the tpa ligand, two iodides, and two methoxide groups. The coordination polyhedron can be described as a highly distorted square antiprism. The U−N distances vary from 2.579(3) to 2.716(3) Å with the shortest distance observed for one of the pyridyl nitrogens. The mean value of the U−N distances (2.68(7) Å) is longer than the one found for the

---

(48) Zalkin, A.; Edwards, P. G.; Zhang, D.; Andersen, R. A. *Acta Crystallogr., Sect. C: Cryst. Struct. Commun.* **1986**, *42*, 1480.

(49) Roussel, P.; Alcock, N. W.; Boaretto, R.; Kingsley, A. J.; Munslow, I. J.; Sanders, C. J.; Scott, P. *Inorg. Chem.* **1999**, *38*, 3651.

(50) Roussel, P.; Hitchcock, P. B.; Tinker, N. D.; Scott, P. *Inorg. Chem.* **1997**, *36*, 5716.

(51) Cuellar, E. A.; Marks, T. J. *Inorg. Chem.* **1981**, *20*, 2129.

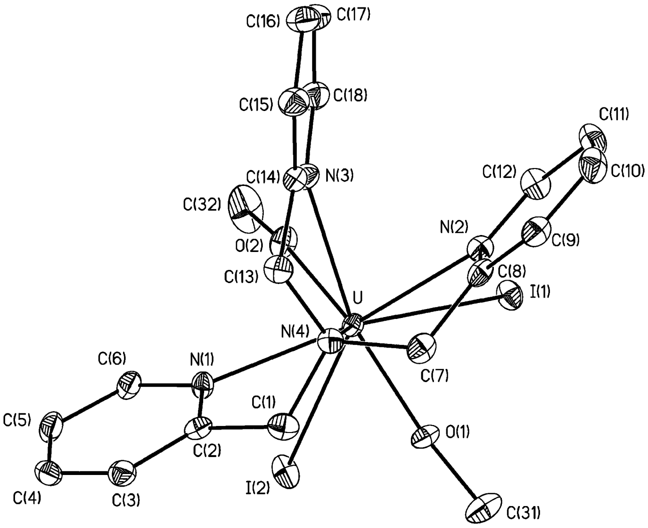

Figure 8. Top view of the molecular structure of the complex [U(tpa)-$(OMe)_2I_2$], with thermal ellipsoids at 30% probability.

Table 6. Selected Bond Lengths (Å) and Angles (deg) for **5**

U−O(1)	2.0619(19)	U−N(4)	2.715(3)
U−O(2)	2.072(2)	U−N(3)	2.716(3)
U−N(1)	2.579(3)	U−I(1)	3.1670(3)
U−N(2)	2.711(3)	U−I(2)	3.2634(3)
C(31)−O(1)−U	153.2(2)	C(32)−O(2)−U	160.2(3)
O(1)−U−O(2)	155.54(9)	N(4)−U−N(3)	62.25(8)
O(1)−U−N(1)	94.97(9)	O(1)−U−I(1)	84.01(7)
O(2)−U−N(1)	88.95(9)	O(2)−U−I(1)	83.02(7)
O(1)−U−N(2)	80.03(8)	N(1)−U−I(1)	156.82(6)
O(2)−U−N(2)	117.21(9)	N(2)−U−I(1)	78.15(6)
N(1)−U−N(2)	124.59(8)	N(4)−U−I(1)	138.84(6)
O(1)−U−N(4)	74.87(8)	N(3)−U−I(1)	114.48(6)
O(2)−U−N(4)	127.34(8)	O(1)−U−I(2)	77.77(6)
N(1)−U−N(4)	61.71(8)	O(2)−U−I(2)	80.18(6)
N(2)−U−N(4)	63.81(8)	N(1)−U−I(2)	73.87(6)
O(1)−U−N(3)	132.12(8)	N(2)−U−I(2)	152.36(5)
O(2)−U−N(3)	72.31(9)	N(4)−U−I(2)	124.48(6)
N(1)−U−N(3)	83.28(8)	N(3)−U−I(2)	144.38(6)
N(2)−U−N(3)	63.07(8)	I(1)−U−I(2)	83.331(7)

monomethoxo complex **4** probably due to the additional sterical hindrance resulting from the substitution of one iodide with one methoxide. This ligand substitution leads also to the complete disruption of the C_3 symmetry of the tpa ligand. The U−OMe distance in both complexes (U−O(1) = 2.027(2) Å in complex **4** and U−O(1) = 2.062(2) Å, U−O(2) = 2.072(2) Å in complex **5**) is considerably shorter than those in a range of alkoxo and phenoxo compounds (2.23−2.15 Å),[46,47,50,52] but is similar to those found for the monophenoxo complex [$Ucp_2(Cl)(OC_6H_3Pr^i{}_2$-2,6)] (U−O = 2.061(8))[53] and for the methoxo complex [$cp_2U(OMe)]_2PH$ (2.046(14) Å).[54] The values of the U−O−C angles are 153.2(2)° for O(1) and 160.2(3)° for O(2) in complex **5**, and 161.28(17)° in complex **4**. The short U−O bond length and the large U−O−C angles observed in complexes **4** and **5** could indicate the presence of a π-bonding between the oxygen lone pairs and empty metal based orbitals in these complexes.

Conclusion

This study highlights the influence of the coordination environment on the reactivity of U(III) complexes in oxidation chemistry. In particular the complex [$U(tpa)_2]I_3$ has been shown to be much more reactive toward water oxidation than U(III) complexes containing cyclopentadienyl derivatives. While for cyclopentadienyl derivatives the stoichiometric reaction with water leads to a hydroxo complex of U(III) which only at high temperature (373 K) decomposes to give U(IV) oxo species, the reaction of [$U(tpa)_2]I_3$ with stoichiometric amounts of water at room temperature results in the formation of a U(IV) trimeric oxo complex. The reaction of U(III) with methanol in the presence of the supporting ligand tpa leads to formation of alkoxo complexes, similarly to what is found for amide or cyclopentadienyl derivatives. However, for cyclopentadienyl derivatives a different mechanism has been suggested for the oxidation reaction, involving a proton-transfer reaction followed by valence disproportionation reactions instead of hydrogen formation. The investigation of the oxidation reaction with different one-electron oxidants is in progress in order to further assess the influence of the presence of neutral heterocyclic amines as supporting ligands on the metal reactivity.

This study also uncovers a suitable route to monomeric aliphatic alkoxo complexes which does not involve the formation of alkaline salts. The potential of this synthetic route is under investigation with other alkoxides and phenoxides.

Acknowledgment. This work was supported by the Commissariat à l'Energie Atomique, Direction de l'Energie Nucléaire. We thank Pierre-Alain Bayle for the help in recording the NMR spectra.

Supporting Information Available: Crystallographic data in CIF format for compounds **1**−**5** and for the protonated ligand $tpaH_3I_3$. Proton NMR spectra of intermediates in the reaction of the bis(tpa) complex with water and with methanol (S1, S2). This material is available free of charge via the Internet at http://pubs.acs.org.

IC0343004

---

(52) Cotton, F. A.; Marler, O. D.; Schwotzer, W. *Inorg. Chem.* **1984**, *23*, 4211.

(53) Blake, P. C.; Lappert, M. F.; Taylor, R. G.; Atwood, J. L.; Zhang, H. *Inorg. Chim. Acta* **1987**, *139*, 13.

(54) Duttera, M. R.; Day, V. W.; Marks, T. J. *J. Am. Chem. Soc.* **1984**, *106*, 2907.